Pulsar Timing with the Parkes Radio Telescope for the *Fermi* Mission

P. Weltevrede[A], *S. Johnston*[A,F], *R. N. Manchester*[A], *R. Bhat*[B], *M. Burgay*[C],
D. Champion[A], *G. B. Hobbs*[A], *B. Kızıltan*[D], *M. Keith*[A], *A. Possenti*[C],
J. E. Reynolds[A], *and K. Watters*[E]

[A] Australia Telescope National Facility, CSIRO, PO Box 76, Epping, NSW 1710
[B] Centre for Astrophysics and Supercomputing, Swinburne University of Technology,
 Mail H39, PO Box 218, Hawthorn, Vic 3122
[C] INAF-Osservatorio Astronomico di Cagliari, I-09012 Capoterra, Italy
[D] Dept of Astronomy & Astrophysics, University of California & UCO Lick Observatory,
 Santa Cruz, CA 95064, USA
[E] Dept of Physics, Stanford University, Stanford, CA 94305, USA
[F] Corresponding author. Email: Simon.Johnston@csiro.au

Abstract: We report here on two years of timing of 168 pulsars using the Parkes radio telescope. The vast majority of these pulsars have spin-down luminosities in excess of 10^{34} erg s^{-1} and are prime target candidates to be detected in gamma-rays by the *Fermi* Gamma-Ray Space Telescope. We provide the ephemerides for the ten pulsars being timed at Parkes which have been detected by *Fermi* in its first year of operation. These ephemerides, in conjunction with the publicly available photon list, can be used to generate gamma-ray profiles from the *Fermi* archive. We will make the ephemerides of any pulsars of interest available to the community upon request. In addition to the timing ephemerides, we present the parameters for 14 glitches which have occurred in 13 pulsars, seven of which have no previously known glitch history. The Parkes timing programme, in conjunction with *Fermi* observations, is expected to continue for at least the next four years.

1 Introduction

The *Fermi* Gamma-Ray Space Telescope, launched in 2008 June, has the study of pulsars at gamma-ray wavelengths as one of its key science projects. *Fermi* follows in the footsteps of its predecessor, the Compton Gamma-Ray Observatory (CGRO) which was active during the 1990s. CGRO detected seven gamma-ray pulsars (including the radio-quiet pulsar Geminga) with three other possible detections (including a millisecond pulsar). CGRO relied on ephemerides for the pulsars it observed in order to correctly phase tag the received gamma-ray photons to produce a light curve. Three of the pulsars detected by CGRO (PSRs B1706−44, B1055−52 and B1509−58) used data obtained with the Parkes radio telescope (Thompson et al. 1992; Fierro et al. 1993; Ulmer et al. 1993; Johnston et al. 1995).

The Large Area Telescope (LAT) on board *Fermi* (Atwood et al. 2009) has a field of view which is substantially bigger than that of the Energetic Gamma-Ray Experiment Telescope (EGRET) aboard CGRO, has a sensitivity more than an order of magnitude greater, far superior energy resolution and a positional accuracy measured in arcmin rather than degrees. *Fermi* began sky-survey observations on 2008 August 11 and in survey mode observes the entire sky every three hours. The

characteristics of the photons received by *Fermi* remained proprietary for the first year of operation but full data release occurred in 2009 August.

In principle, therefore, *Fermi* can produce light curves for every pulsar in the sky and update the profile on a daily basis. To produce these profiles for all but a handful of the brightest pulsars, generally requires an accurate pulsar ephemeris so that the incoming photons can be correctly phase tagged. Prior to the launch of *Fermi*, the worldwide radio pulsar timing community formalised a comprehensive pulsar monitoring campaign using the Parkes, Lovell, Nançay, Green Bank and Arecibo telescopes (Smith et al. 2008). The time pressure on these large telescopes means that it is not possible to time all of the ∼2000 known pulsars. The timing list created by Smith et al. (2008) contained 224 pulsars with a spin-down energy loss rate, $\dot{E}$, larger than 10^{34} erg s^{-1}. Of these 224 pulsars, 156 are timed at Parkes.

One of the major issues facing the radio timing campaign is that many of the pulsars potentially detectable by *Fermi* are young, high $\dot{E}$ objects. These pulsars are far from perfect clocks and suffer from a high degree of timing noise (Hobbs et al. 2004). In order to track the timing noise to a level of accuracy sufficient to time-tag the photons to 10^{-2}–10^{-3} of the rotational period, we

need to observe the entire sample approximately once per month.

Fermi has been a spectacular success since its launch. It has discovered 16 gamma-ray pulsars through 'blind' periodicity searches (Abdo et al. 2009d) of which two have subsequently been detected in the radio (Camilo et al. 2009). In addition it has produced high quality profiles for 8 millisecond radio pulsars (Abdo et al. 2009e) and more than 20 'normal' (non-millisecond) pulsars, including the Crab pulsar (Abdo et al. 2010a), the Vela pulsar (Abdo et al. 2009f), the recently discovered PSR J1028−5819 (Keith et al. 2008; Abdo et al. 2009a) and 6 pulsars with moderate $\dot{E}$ (Weltevrede et al. 2009). All these results have been tabulated in the gamma-ray pulsar catalogue (Abdo et al. 2010b).

The radio data obtained through the pulsar timing program has a number of other applications, including a statistical determination of the alignment of the magnetic and rotational axis as a function of time (Weltevrede & Johnston 2008a) and examination of the polarisation characteristics of highly energetic pulsars (Weltevrede & Johnston 2008b). In addition, long term radio timing shows that a number of pulsars glitch (Shemar & Lyne 1996; Wang et al. 2000; Janssen & Stappers 2006) and the glitch parameters and time between events can be used to determine the interior structure of neutron stars (Ruderman, Zhu & Chen 1998).

Of the 'normal' radio pulsars detected by *Fermi*, Parkes is responsible for timing ten of them. In this paper we describe the Parkes timing campaign for the *Fermi* mission, including the observational and data analysis details. We provide the timing ephemerides for, and a brief discussion of, the 10 pulsars detected by *Fermi*. We tabulate the glitches seen in the monitored pulsars during the two years of the timing program. We briefly discuss the implications of the results and the next steps for the *Fermi* mission.

2 Observations and Data Analysis

Observations in support of the *Fermi* mission commenced in 2007 February. All observations were carried out using the 64-m radio telescope in Parkes, NSW, Australia. Generally, each observing session used an observing frequency near 1.4 GHz and lasted 24 h with the observing sessions separated by approximately 4 weeks. However, once every six months we had an extended observing session and data were obtained at both 3.1 and 0.7 GHz in order to monitor long-term dispersion measure variations. Each pulsar is typically observed for only a few minutes, sufficient to reach a signal-to-noise ratio greater than 5. A total of 156 pulsars from the Smith et al. (2008) list are timed at Parkes; their basic parameters are given in Table 1, which gives the parameters and post-fit rms taken from Smith et al. (2008) and observed at Parkes in support of the *Fermi* mission. A further 12 pulsars are also timed; these are listed separately in Table 2.

At 1.4 GHz, we used the centre beam of the multibeam receiver (Staveley-Smith et al. 1996) with a total

bandwidth of 256 MHz. The noise-equivalent flux density of the system is ∼35 Jy on cold sky. For the 3.1 GHz and 0.7 GHz observing, data were recorded simultaneously using the dual 10/50-cm receiver (Granet et al. 2005) with a usable bandwidth of 1024 and 40 MHz respectively. The noise-equivalent flux density is ∼49 Jy at 3.1 GHz and 70 Jy at 0.7 GHz. Many pulsars in our sample are located in the Galactic plane where the sky temperature can be up to ∼50 K at 1.4 GHz and several hundred K at 0.7 GHz, substantially raising the noise-equivalent flux density on these sources.

The downconverted signals from each polarisation channel of the linear feeds were fed in a digital filterbank, designed and built at the Australia Telescope National Facility. The hardware converts the analogue voltages into digital signals and produces a filterbank output consisting of 1024 frequency channels for each of 1024 phase bins across the pulse period for the two auto correlations and real and imaginary parts of the cross correlations of the feed probes. Data were folded at the topocentric pulse period and accumulated for 30 s and then dumped to disk. A calibration signal, injected into the feed at an angle of 45° to the probes, was recorded on a regular basis. This signal is used to determine the relative gain of the two polarisation channels and the phase between them.

Data analysis was carried out using the PSRCHIVE package (Hotan, van Straten & Manchester 2004). In brief, after removal of interference in both the frequency and time domains, the data are gain and polarisation calibrated and summed in frequency and time to produce a pulse profile for each pulsar observed.

3 Pulsar Timing

In order to produce a time-of-arrival (TOA) the resultant pulse profile is cross correlated with a high signal-to-noise ratio 'standard' profile. The standard profile is created by summing together all previous observations of the pulsar using a technique described in detail in Weltevrede & Johnston (2008b). The topocentric TOA at the weighted centre frequency of the observation is then added to the database of previous TOAs obtained for this pulsar.

Pulsar timing is carried out using the TEMPO2 package (Hobbs, Edwards & Manchester 2006). In addition to other auxiliary files, TEMPO2 requires a model for the spin behaviour of the pulsar and the database of TOAs. After converting the TOAs to the solar system barycentre using the DE405 model (Standish 1998; Edwards, Hobbs & Manchester 2006), TEMPO2 compares the TOAs to the model predictions to produce a set of residuals. These residuals are then used to refine the initial input model.

Assuming we have an accurate pulsar position obtained through other means, the first step to determining a timing solution is to fit only for the pulsar spin frequency, ν, and frequency derivative, $\dot{\nu}$. This effectively removes linear and quadratic terms from the residuals; what remains is then generally dominated by a cubic term. In these young pulsars, this cubic term is generally many orders of magnitude larger than the frequency second derivative

Table 1. Parameters and post-fit RMS in milli-periods (mP)

Name	P (ms)	DM (pc cm^{-3})	log $\dot{E}$ (erg s^{-1})	rms (mP)
J0543+2329	246.0	78	34.6	1.1
J0614+2229	335.0	97	34.8	3.3
J0627+0705	475.9	138	34.0	0.4
J0659+1414	384.9	14	34.6	3.2
J0729−1448	251.7	92	35.4	5.3
J0742−2822	166.8	74	35.1	0.9
J0745−5353	214.8	122	34.0	4.2
J0821−3824	124.8	196	34.7	1.9
J0834−4159	121.1	240	35.0	3.9
J0835−4510	89.4	68	36.8	2.3
J0855−4644	64.7	238	36.0	12.0
J0857−4424	326.8	184	34.4	1.4
J0901−4624	442.0	199	34.6	0.6
J0905−5127	346.3	196	34.4	0.4
J0908−4913	106.8	180	35.7	0.5
J0940−5428	87.5	134	36.3	4.5
J0954−5430	472.8	200	34.2	0.7
J1003−4747	307.1	98	34.5	0.5
J1015−5719	139.9	279	35.9	4.8
J1016−5819	87.8	252	34.6	2.0
J1016−5857	107.4	394	36.4	3.2
J1019−5749	162.5	1039	35.3	8.0
J1020−6026	140.5	445	35.0	12.9
J1043−6116	288.6	449	34.2	0.5
J1048−5832	123.7	129	36.3	5.3
J1052−5954	180.6	491	35.1	12.1
J1055−6032	99.7	633	36.0	−
J1057−5226	197.1	30	34.5	0.3
J1105−6107	63.2	271	36.4	5.2
J1112−6103	65.0	599	36.7	10.5
J1115−6052	259.8	228	34.2	0.7
J1119−6127	407.7	707	36.4	0.2
J1123−6259	271.4	223	34.0	0.9
J1124−5916	135.3	330	37.1	−
J1138−6207	117.6	520	35.5	4.9
J1156−5707	288.4	244	34.6	0.7
J1216−6223	374.0	787	34.1	4.4
J1224−6407	216.5	97	34.3	0.3
J1248−6344	198.3	433	34.9	8.0
J1301−6305	184.5	374	36.2	14.0
J1302−6350	47.8	147	35.9	2.8
J1305−6203	427.8	470	34.2	2.0
J1320−5359	279.7	98	34.2	0.5
J1327−6400	280.7	681	34.7	8.1
J1341−6220	193.3	717	36.1	3.7
J1349−6130	259.4	285	34.1	0.9
J1357−6429	166.1	128	36.5	7.0
J1359−6038	127.5	294	35.1	0.2
J1406−6121	213.1	542	35.3	9.4
J1412−6145	315.2	515	35.1	3.6
J1413−6141	285.6	677	35.7	89.7
J1420−6048	68.2	360	37.0	16.7
J1452−5851	386.6	262	34.5	2.2
J1452−6036	155.0	350	34.2	0.4
J1453−6413	179.5	71	34.3	0.6
J1509−5850	88.9	138	35.7	12.1
J1512−5759	128.7	629	35.1	0.9
J1513−5908	150.7	252	37.3	11.2
J1514−5925	148.8	194	34.5	3.2
J1515−5720	286.6	482	34.0	1.5
J1524−5625	78.2	153	36.5	5.3
J1524−5706	1116.0	833	34.0	0.6

(Continued)

Table 1.   (Continued)

Name	P (ms)	DM (pc cm^{-3})	log $\dot{E}$ (erg s^{-1})	rms (mP)
J1530−5327	279.0	50	33.9	0.8
J1531−5610	84.2	111	36.0	1.5
J1538−5551	104.7	603	35.0	8.4
J1539−5626	243.4	176	34.1	0.9
J1541−5535	295.8	428	35.0	5.3
J1543−5459	377.1	346	34.6	1.9
J1548−5607	170.9	316	34.9	1.8
J1549−4848	288.3	56	34.4	1.2
J1551−5310	453.4	493	34.9	7.1
J1600−5044	192.6	261	34.4	0.4
J1600−5751	194.5	177	34.0	0.9
J1601−5335	288.5	195	35.0	9.4
J1611−5209	182.5	128	34.5	0.3
J1614−5048	231.7	583	36.2	5.6
J1617−5055	69.4	467	37.2	−
J1626−4807	293.9	817	34.4	17.8
J1627−4706	140.7	456	34.4	9.4
J1632−4757	228.6	578	34.7	7.8
J1632−4818	813.5	758	34.7	12.8
J1637−4553	118.8	193	34.9	0.9
J1637−4642	154.0	417	35.8	9.9
J1638−4417	117.8	436	34.6	4.0
J1638−4608	278.1	424	35.0	0.9
J1640−4715	517.4	592	34.1	3.7
J1643−4505	237.4	484	35.0	2.4
J1646−4346	231.6	490	35.6	6.2
J1648−4611	165.0	393	35.3	6.2
J1649−4653	557.0	332	34.0	1.6
J1650−4502	380.9	320	34.0	2.0
J1650−4921	156.4	230	34.3	1.0
J1702−4128	182.1	367	35.5	6.5
J1702−4305	215.5	538	34.6	5.9
J1702−4310	240.5	377	35.8	4.1
J1705−3950	318.9	207	34.9	2.0
J1709−4429	102.5	76	36.5	4.6
J1715−3903	278.5	313	34.8	5.7
J1718−3825	74.7	247	36.1	3.0
J1721−3532	280.4	496	34.7	1.0
J1722−3712	236.2	100	34.5	1.7
J1723−3659	202.7	254	34.6	1.1
J1726−3530	1110.3	727	34.5	6.3
J1730−3350	139.5	259	36.1	1.3
J1731−4744	829.8	123	34.0	0.4
J1733−3716	337.6	154	34.2	1.0
J1734−3333	1169.2	578	34.7	9.6
J1735−3258	351.0	754	34.4	14.9
J1737−3137	450.4	488	34.8	4.2
J1738−2955	443.4	223	34.6	0.9
J1739−2903	322.9	139	34.0	0.3
J1739−3023	114.4	170	35.5	5.8
J1740−3015	606.8	152	34.9	9.6
J1745−3040	367.4	88	33.9	0.7
J1756−2225	405.0	326	34.5	1.1
J1757−2421	234.1	179	34.6	0.4
J1801−2154	375.3	388	34.1	3.1
J1801−2304	415.8	1074	34.8	4.0
J1801−2451	124.9	289	36.4	4.9
J1803−2137	133.6	234	36.3	6.5
J1806−2125	481.8	750	34.6	3.8
J1809−1917	82.7	197	36.3	5.3
J1812−1910	431.0	892	34.3	9.0
J1815−1738	198.4	728	35.6	3.3

(Continued)

Table 1.   (Continued)

Name	P (ms)	DM (pc cm^{-3})	log $\dot{E}$ (erg s^{-1})	rms (mP)
J1820−1529	333.2	772	34.6	5.5
J1824−1945	189.3	225	34.5	0.3
J1825−1446	279.2	357	34.6	1.7
J1826−1334	101.5	231	36.4	7.7
J1828−1057	246.3	245	34.7	6.7
J1828−1101	72.1	607	36.2	5.1
J1830−1059	405.0	162	34.6	1.0
J1831−0952	67.3	247	36.0	6.3
J1832−0827	647.3	301	34.0	0.7
J1833−0827	85.3	411	35.8	1.7
J1834−0731	513.0	295	34.2	4.3
J1835−0643	305.8	473	34.7	4.6
J1835−0944	145.3	277	34.7	5.9
J1835−1106	165.9	133	35.3	2.4
J1837−0559	201.1	318	34.2	4.4
J1837−0604	96.3	462	36.3	17.1
J1838−0453	380.8	621	34.9	2.8
J1838−0549	235.3	274	35.0	4.3
J1839−0321	238.8	449	34.6	4.1
J1839−0905	419.0	348	34.1	1.9
J1841−0425	186.1	325	34.6	0.5
J1841−0524	445.7	289	35.0	4.6
J1842−0905	344.6	343	34.0	1.1
J1843−0355	132.3	798	34.3	12.4
J1843−0702	191.6	228	34.1	2.6
J1844−0256	273.0	820	34.7	23.7
J1844−0538	255.7	413	34.4	1.1
J1845−0743	104.7	281	34.1	0.3
J1847−0402	597.8	142	34.0	0.7
J1853+0011	397.9	569	34.3	2.9
J1853−0004	101.4	438	35.3	1.6
J1903+0925	357.2	162	30.7	−

Table 2.   Parameters and post-fit RMS in milli-periods (mP)[a]

Name	P (ms)	DM (pc cm^{-3})	log $\dot{E}$ (erg s^{-1})	rms (mP)
J0108−1431	807.6	2	30.8	0.5
J0401−7608	545.3	22	32.6	1.0
J0536−7543	1245.9	18	31.1	0.4
J0630−2834	1244.4	34	32.2	1.2
J0738−4042	374.9	161	33.1	0.6
J1028−5819	91.4	97	35.9	0.4
J1456−6843	263.4	9	32.3	15.9
J1602−5100	864.2	171	33.6	0.9
J1638−4725	763.9	550	32.4	52.1
J1705−1906	299	23	33.8	0.3
J1825−0935	769	19	33.7	0.9
J1845−0434	486.8	231	33.6	0.8

[a]In addition to those contained in Smith et al. (2008).

expected from a simple dipole braking model and is the result of timing noise or glitch recovery (e.g. Johnston & Galloway 1999). Although one can, in principle, continue to fit higher order polynomials to the data in order to whiten them, a different technique is used.

The technique (developed by Hobbs et al. 2004) instead removes harmonically related sinusoids from the residual data after fitting for ν and $\dot{\nu}$ and continues to remove components until the residuals resemble white noise. This whitening technique is implemented using the FITWAVES algorithm within TEMPO2.

An added complication arises if the pulsar suffers a glitch. A glitch causes an abrupt change in both ν and $\dot{\nu}$ and the magnitude of the change can be large. With

sparsely sampled data it is very difficult to maintain phase coherence through the epoch of the glitch. This implies that the glitch epoch cannot be well determined — in the case of our data, we generally cannot determine the glitch epoch to better than ~15 days. In order to measure the glitch parameters, we determine a timing solution before and after the glitch and then, using the two solutions, estimate $\Delta\nu$ and $\Delta\dot{\nu}$. With these estimates, and by setting the glitch epoch midway between the observation just before and just after the glitch, a timing solution can be obtained for the entire data set with the addition of a phase jump at the glitch epoch.

One of the important parameters to measure, in the context of models of gamma-ray emission, is the offset between the radio and gamma-ray profiles. In order to do this, an accurate value of the dispersion measure (DM) is needed so that the dispersion delay between the ~1 GHz radio profile and the ~GeV gamma-ray profile can be corrected for. We measured the DM across the 256 MHz bandwidth at 1.4 GHz assuming no profile evolution across the band which is generally sufficient to determine the DM to ~0.01 cm^{-3} pc. This corresponds to an uncertainty of ~40 μs in the offset between the radio and gamma-ray profiles.

4 Results: General Timing

In the last columns of Tables 1 and 2 we list the rms of the residuals in milli-periods for each pulsar following fitting for ν, $\dot{\nu}$ and whitening if necessary. When creating gamma-ray profiles from the radio ephemeris, the rms constrains the maximum useful number of phase bins across the light curve. The rms is less than 2 milli-periods for 64 pulsars in our sample — 500 bins across the light curve is then possible. Only for 18 pulsars is the rms worse than 10 milli-periods. We note that the accuracy of the time tagging of the gamma-ray photons is significantly better than 1 μs (Smith et al. 2008) and is not a limiting factor in the time-resolution of the resulting gamma-ray profiles. Typically, the small number of photons received from gamma-ray pulsars limits the profile resolution to less than 100 bins.

In three cases we have been unable to maintain phase coherence in the timing data. The pulsars concerned are PSRs J1055−6032, J1617−5055 and J1903+0925. In the latter case we have less than 1 yr of timing data but the first two named pulsars appear to have extremely large short-term timing noise. They need to be monitored on a much more regular basis than once per month in order to maintain phase coherence. In addition, PSR J1124−5916 is an extremely weak radio pulsar (Camilo et al. 2002) for which it takes ~5 h to obtain a timing point using Parkes and it is therefore not observed as part of our timing programme. Following its detection in gamma-rays by *Fermi* (Abdo et al. 2010b), we observed it on a single occasion in order to phase align the radio and gamma-ray profiles.

5 Results: Glitches

We have detected 14 glitches in 13 of the pulsars in our sample. These glitches are tabulated in Table 3 with

Table 3. Parameters of the 14 glitches observed in the timing data

Name	Epoch (MJD)	$\Delta\nu/\nu$ ($\times10^{-6}$)	$\Delta\dot{\nu}/\dot{\nu}$ ($\times10^{-3}$)
J0729−1448[†]	54711(21)	6.6203(4)	13.86(5)
J1048−5832	54495(10)	3.0431(2)	4.77(2)
J1052−5954[†]	54526(22)	6.7478(7)	14.1(4)
J1105−6107	54711(21)	0.023(1)	0.0(3)
J1341−6220	54468(18)	3.0782(3)	
	54870(11)	3.0667(3)	
J1357−6429	54803(17)	1.752(7)	2.8(2.8)
J1410−6132[†]	54652(19)	0.2726(5)	−3.31(5)
J1420−6048[†]	54652(20)	0.9371(3)	2.95(1)
J1709−4429	54710(22)	2.7497(1)	4.95(1)
J1737−3137[†]	54352.3(1.0)	1.3425(4)	0.4(6)
J1740−3015[†]	54468(17)	0.037(1)	−0.4(4)
J1801−2451	54680(9)	3.0904(2)	5.04(2)
J1841−0524[†]	54495(10)	1.0359(4)	0.11(15)

[†]Pulsar not previously known to have glitched.

the parameters estimated using the scheme outlined in Section 3. The epoch of the glitch is set at the midpoint between the last pre-glitch and first post-glitch data point. We note that *Fermi* data can be used to better constrain the glitch epoch for PSR J1709−4429 (Abdo et al. 2009c). The third column of the table gives the fractional change in the spin frequency, $\Delta\nu/\nu$ and the final column lists the fractional change in the frequency derivative, $\Delta\dot{\nu}/\dot{\nu}$. The listed errors are twice the formal errors given by TEMPO2 and given in brackets which refer to the last digit(s). Three of the pulsars in the table have been detected by *Fermi*. For PSRs J1048−5832 and J1420−6048 the glitch occurred prior to the launch of the satellite. The glitch in PSR J1709−4429 happened shortly after *Fermi* began its all sky survey in 2008 August.

Of the 13 pulsars, 7 have not previously been known to glitch, these are listed with the † symbol in Table 3. The other 6 pulsars have previously been observed to glitch as tabulated in the compilation of Wang et al. (2000). Most notable is PSR J1341−6220 (B1338−62) which has the shortest average interval between glitches of any pulsar, estimated by Wang et al. (2000) to be 250 days. In the 800 days of our timing data we see two glitches separated by some 400 days. Both glitches have about the same magnitude and are larger than any of the other 12 glitches reported for this pulsar. There is not sufficient time between the glitches to determine a reliable value of $\Delta\dot{\nu}/\dot{\nu}$. PSR J1740−3015 (B1737−30) is another pulsar which glitches often (Zou et al. 2008) and we have detected one relatively small glitch in this object.

The smallest glitch we report here has $\Delta\nu/\nu$ of 2×10^{-8} and we believe our sample to be complete above a limit of about 10^{-8}. Below this limit it is very hard, with our data set, to distinguish between glitches and timing noise. We attempted to fit glitch parameters to possible 'cuspy' looking residuals, similar to those seen in

Table 4. Timing Parameters for 5 Pulsars Detected in Gamma-Rays by *Fermi*

Parameters	J0659+1414	J0742−2822	J0835−4510	J1028−5819	J1048−5832
Right Ascension (J2000)	06:59:48.134	07:42:49.026	08:35:20.61149	10:28:27.95	10:48:12.2
Declination (J2000)	+14:14:21.5	−28:22:43.70	−45:10:34.8751	−58:19:05.225	−58:32:05.8
Spin frequency, ν (s^{-1})	2.598136794(2)	5.996283159(8)	11.191119(5)	10.9404949958(3)	8.08398924(6)
$\dot{\nu}$ (10^{-15})	−370.981(5)	−611(7)	−15600(170)	−1928.4(3)	−6259(7)
DM (cm^{-3} pc)	13.7(2)	73.790(3)	67.9754(8)	96.39(9)	128.822(8)
Proper motion in RA (mas yr^{-1})	44.07	−29	−49.68		
Proper motion in Dec (mas yr^{-1})	−2.4	4	29.9		
Epoch (MJD)	49721.0	54615.0	54217.0	54787.0	54615.0
Ref. MJD	54762.6946809825	54632.9827544637	54606.2500568554	54786.6818285185	54606.2571751136
Ref. freq (MHz)	1369.235	1377.652	1373.864	1374.656	1373.864
Glitch epoch (MJD)					54490
Glitch phase offset					−0.484(6)
Glitch $\Delta\nu$ (10^{-5})					2.4616(3)
Glitch $\Delta\dot{\nu}$ (10^{-14})					−3.7(4)
Start (MJD)	54505	54220	54207	54563	54220
Finish (MJD)	55011	55010	55010	55011	55011
Wave frequency (rad day^{-1})		0.0063560	0.0052116	0.0093621	0.0059587
Wave 1		−0.4498,+0.05777	+3.318,−1.538	−0.008672,−0.002189	−0.3531,−0.1548
Wave 2		+0.09547,−0.02979	+0.1863,−1.021	+0.002582,−0.001674	+0.07018,+0.01160
Wave 3		−0.03240,+0.0167	−0.3375,−0.2816	−0.0002706,−3.2135e−05	−0.01741,−0.004765
Wave 4		+0.01348,−0.009575	−0.1746,+0.08070		+0.007688,+0.0005985
Wave 5		−0.004789,+0.005083	+0.003159,+0.07619		−0.001823,+0.002077
Wave 6		+0.001260,−0.002011	+0.02241,+0.007917		
Wave 7		−0.0003854,+0.0008335	+0.003275,−0.003641		

Table 4. (Continued)

| Parameters	J1057−5226	J1420−6048	J1509−5850	J1709−4429	J1718−3825
Right Ascension (J2000)	10:57:58.84	14:20:08.237	15:09:27.13	17:09:42.728	17:18:13.565
Declination (J2000)	−52:26:56.3	−60:48:16.43	−58:50:56.1	−44:29:08.24	−38:25:18.06
Spin frequency, ν (s^{-1})	5.0732274494(7)	14.66248295(6)	11.2455254698(1)	9.7565189994(9)	13.391571381(4)
$\dot{\nu}$ (10^{-15})	−150.4(6)	−17710(16)	−1159.23(1)	−8831.0(7)	−2375(4)
Epoch (MJD)	54615.0	54615.0	54615.0	54616.0	54616.0
DM (cm^{-3} pc)	30.1	360	137.7	75.69	247.4
Ref. MJD	54606.2654505538	54633.2224514535	54633.2560188871	54633.4457155762	54633.4498848905
Ref. freq (MHz)	1373.864	1377.652	1377.652	1377.652	1377.652
Glitch epoch (MJD)		54660		54692.8	
Glitch phase offset		−0.23(2)		−0.178(9)	
Glitch $\Delta\nu$ (10^{-5})		1.3659(4)		2.6837(3)	
Glitch $\Delta\dot{\nu}$ (10^{-14})		−10.0(3)		−6.2(1)	
Start (MJD)	54220	54220	54220	54220	54220
Finish (MJD)	55011	55011	55011	55011	55011
Wave frequency (rad day^{-1})	0.0059587	0.0039726	0.0061797	0.0061797	0.0059593
Wave 1	−0.02318,−0.0007458	+5.079,−1.557		+0.06933,−0.2996	−0.3333,+0.007675
Wave 2	+0.005196,+0.0001067	−0.6315,+0.04927		+0.01173,+0.0304	+0.06940,−0.009321
Wave 3	+0.0009044,+0.0004835	+0.08892,−0.007211		−0.002489,−0.001332	−0.02062,+0.006114
Wave 4	+0.0003618,+0.0003014				+0.005628,−0.003100
Wave 5	−0.0001134,−2.68008e−05				−0.0009510,+0.0008923
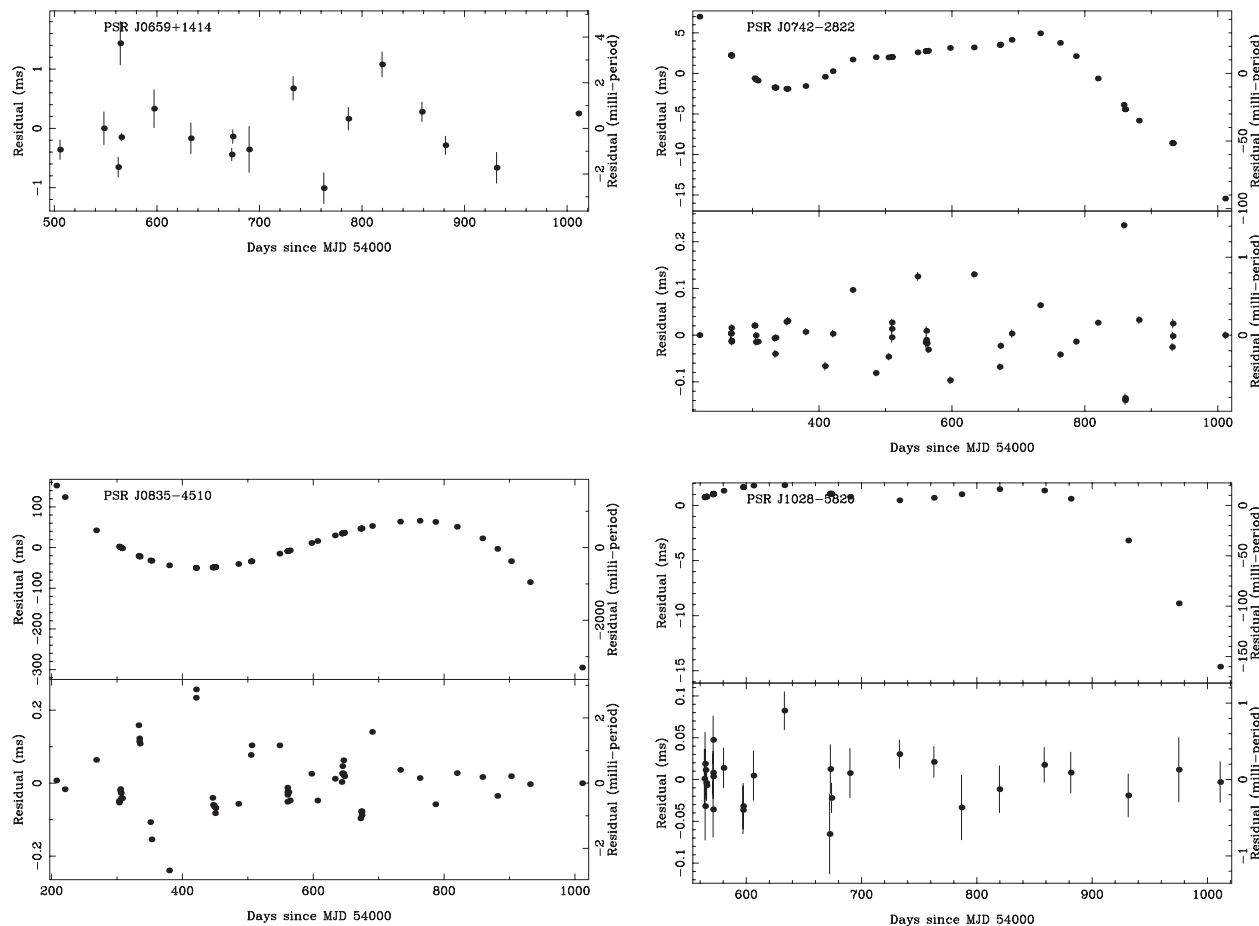
Figure 1 Timing residuals for PSRs J0659+1414 (top left), J0742−2822 (top right), J0835−4510 (bottom left) and J1028−5819 (bottom right). Residuals before (top) and after (bottom) the use of FITWAVES are shown for the latter three pulsars. Note the very different scales on the *y*-axis for these cases.

Janssen & Stappers (2006) for example, but we find that fitting glitches and using FITWAVES return very similar results in spite of their different functional forms.

6 Results: *Fermi* Pulsars

In this section we describe in detail the ten pulsars which have been confirmed as gamma-ray emitters by *Fermi* (Abdo et al. 2010b). We show residuals as a function of time for each pulsar and provide the complete ephemerides in Table 4 and including details of the FITWAVES parameters where appropriate. These ephemerides, in conjunction with the publicly available photon list from *Fermi*, can be used to generate gamma-ray profiles of the *Fermi*-detected pulsars.

We note that for all the pulsars, the clock correction is to TT(TAI), the solar system ephemeris used is DE405, and we are using the barycentric dynamical time (BDT) definition for the spin parameters. For a full description of the meaning of these terms and their implementation in TEMPO2 see Hobbs et al. (2006).

The pulsar's position, proper motion and parallax are held constant during the fitting procedure using the best values taken from the literature. The pulsar's DM is measured across the band at 1.4 GHz and is also held constant

during the fitting. The epoch refers to the epoch at which the rotational frequency and positional parameters are measured. The reference MJD and reference frequency given in the table is the TOA of the fiducial point (the peak of the pulse profile) at the Parkes telescope. Start and finish MJD denote the first and last data points used and hence the range of dates over which the fit is valid. The accuracy of the ephemerides outside the valid MJD range deteriorates quickly in the majority of cases.

PSR J0659+1414/B0656+14 (see Figure 1): This pulsar is a nearby, relatively low $\dot{E}$ pulsar. It is known to produce both thermal and non-thermal X-ray emission (De Luca et al. 2005) and suspected as a gamma-ray pulsator (Ramanamurthy et al. 1996) before confirmation with *Fermi* (Weltevrede et al. 2009). Bright, 'spiky' emission is occasionally seen in the radio pulses (Weltevrede et al. 2006). The pulsar has low timing noise and is not known to have glitched in spite of decades of monitoring. There was no need to whiten the data using FITWAVES as the timing noise is low. Astrometric data are taken from Brisken et al. (2003).

PSR J0742−2822/B0740−28 (see Figure 1): This pulsar was not known as a high-energy emitter until its recent detection with *Fermi* (Weltevrede et al. 2009). It is
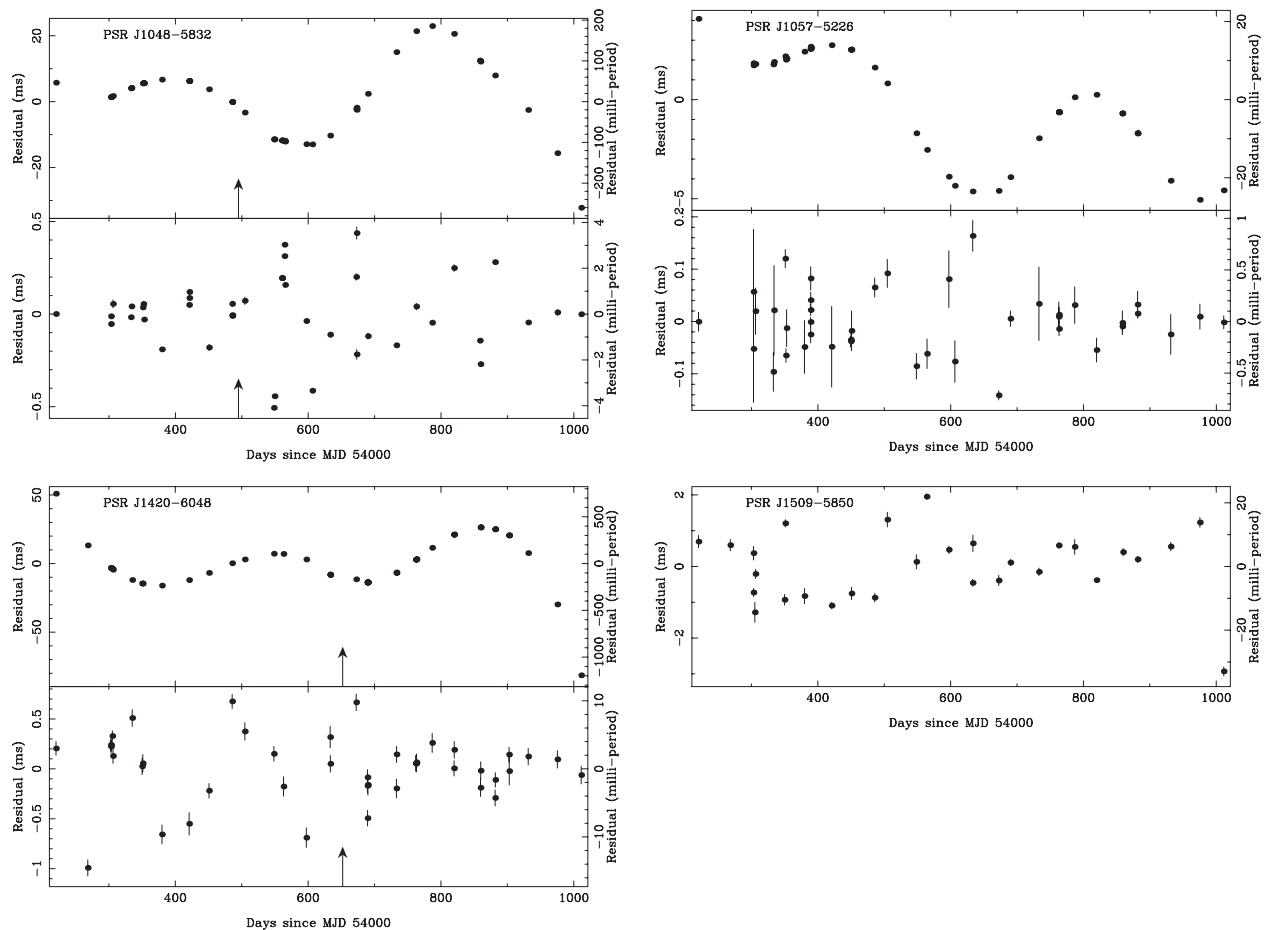
Figure 2 Timing residuals for PSRs J1048−5832 (top left), J1057−5226 (top right), J1420−6048 (bottom left) and J1509−5850 (bottom right). Residuals before (top) and after (bottom) the use of FITWAVES are shown for the latter three pulsars. Note the very different scales on the *y*-axis for these cases. The arrow indicates the epoch of the glitch for PSRs J1048−5832 and J1420−6048.

extremely bright in the radio and the rotation axis appears to point in the direction of its proper motion (Johnston et al. 2005). The pulsar is not known to glitch but suffers a high level of timing noise which was successfully removed with the FITWAVES algorithm. Astrometric data are taken from Fomalont et al. (1997).

PSR J0835−4510/B0833−45 (see Figure 1): The Vela pulsar was one of the first pulsars discovered and has a timing history stretching back over 40 years. Located in the Vela supernova remnant, its gamma-ray pulsations have long been known (Thompson et al. 1975) with the EGRET results discussed in Kanbach et al. (1994) and recent results from the Agile satellite are reported in Pellizoni et al. (2009). *Fermi* has produced beautiful high quality data on this pulsar (Abdo et al. 2009f). Vela suffers glitches on a quasi-regular basis (Wang et al. 2000), but no large glitch has occurred over the timespan of our data. The position, proper motion and parallax for Vela are taken from Dodson et al. (2003).

PSR J1028−5819 (see Figure 1): This pulsar was discovered in 2008 March in a search of unidentified EGRET error boxes (Keith et al. 2008) and subsequently detected as a pulsed gamma-ray emitter by *Fermi* (Abdo et al. 2009a). The very narrow radio profile allows for accurate

TOAs to be obtained and the residual is only 40 µs. The pulsar position is from the interferometric observations of Keith et al. (2008).

PSR J1048−5832/B1046−58 (see Figure 2): This pulsar is a 'Vela-like' object, proposed tentatively as a gamma-ray emitter from EGRET data (Kaspi et al. 2000) and confirmed by *Fermi* (Abdo et al. 2009b). Large pulses are occasionally seen on the rising edge of the profile (Johnston & Romani 2002). The pulsar glitched in early 2008. The timing noise is large and tracks smoothly over the glitch epoch. The pulsar's position is that from Wang et al. (2000).

PSR J1057−5226/B1055−52 (see Figure 2): This pulsar has an interpulse and both the main and interpulses have a complex pulse morphology, described extensively in Weltevrede & Wright (2009). Although it has a relatively low $\dot{E}$, it was seen as a pulsed gamma-ray emitter by EGRET (Fierro et al. 1993). The gamma-ray emission is claimed to be associated with the pole that produces the radio interpulse emission (e.g. Weltevrede & Wright 2009). The timing noise seems quasi-periodic with a period close to one year. The pulsar's position is taken from the radio timing paper of Newton, Manchester & Cooke (1981).
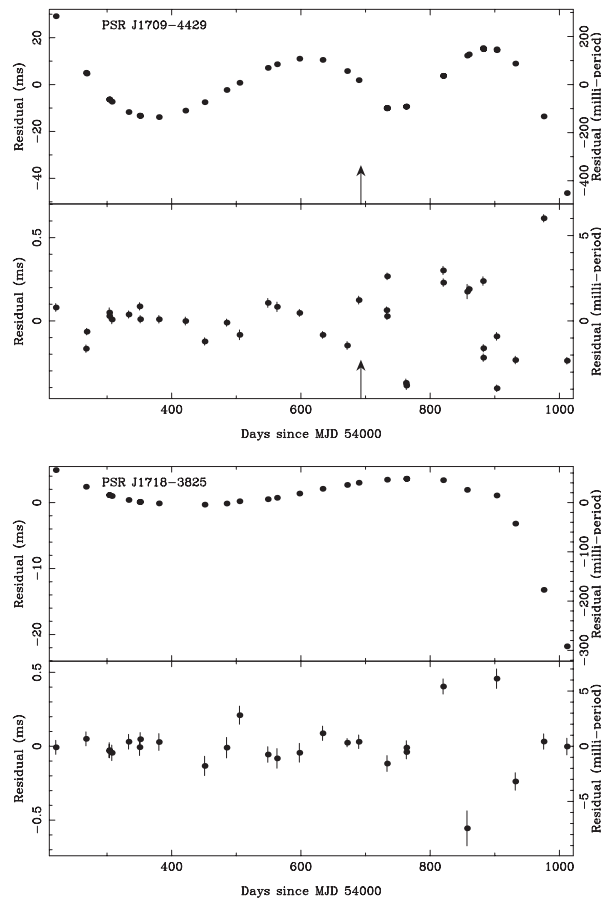
Figure 3 Timing residuals for PSRs J1709−4429 (top), J1718−3825 (bottom). Residuals before (top) and after (bottom) the use of FITWAVES are shown. Note the very different scales on the *y*-axis. The arrow indicates the epoch of the glitch for PSR J1709−4429.

PSR J1420−6048 (see Figure 2): This pulsar lies in a complex region of the Galactic plane and is a known X-ray emitter (Roberts, Romani & Johnston 2001). It was mooted as a possible counterpart to an EGRET unidentified source (D'Amico et al. 2001), and confirmed as a gamma-ray emitter by *Fermi* (Weltevrede et al. 2009). A glitch in the pulsar happened in mid 2008, just before *Fermi* began its all sky survey. The timing noise is large. The pulsar's position is from D'Amico et al. (2001).

PSR J1509−5850 (see Figure 2): The pulsar is located inside an X-ray (Kargaltsev et al. 2008) and radio (Hui & Becker 2007) wind nebula. Weltevrede et al. (2009) report the gamma-ray detection of the pulsar. Its timing noise is very low, the residual after fitting for ν and $\dot{\nu}$ is only 20 milli-periods and there is no need for whitening using FIT-WAVES. The pulsar's position is taken from the discovery paper (Kramer et al. 2003).

PSR J1709−4429/B1706−44 (see Figure 3): This pulsar is a 'Vela-like' object, detected as a gamma-ray emitter by EGRET (Thompson et al. 1992). A glitch occurred in 2008 August; the daily observations and monitoring by *Fermi* allows an accurate epoch to be obtained (Abdo et al. 2009c). The timing noise continues smoothly through the glitch. The pulsar position is that from Wang et al. (2000).

PSR J1718−3825 (see Figure 3): The pulsar has an associated X-ray nebula (Hinton et al. 2007) and a TeV source (Aharonian et al. 2007). The gamma-ray detection of the pulsar is reported in Weltevrede et al. (2009). Its timing noise is relatively large and has a longer timescale than many of the other pulsars in our sample. The pulsar's position is taken from Manchester et al. (2001).

7 Summary

We started a comprehensive program of pulsar timing with the Parkes radio telescope in 2007 February. The launch of the *Fermi* satellite in 2008 June has resulted in the detection of more than 20 (non-MSP) radio pulsars at gamma-ray wavelengths, of which 10 are observed at Parkes. In this paper we have provided the timing ephemerides for the 10 pulsars, which, in conjunction with the publicly available photon parameters from *Fermi*, allow a recreation of the gamma-ray profiles. In addition we have detected 14 glitches in 13 different pulsars and provide the glitch parameters.

The *Fermi* mission will continue for at least a further 4 years and we plan to carry out the pulsar timing for a similar length of time. Researchers who require ephemerides from any of the pulsars contained in Table 1 can contact the authors of this paper.

References

Abdo, A. A. et al., 2009a, ApJ, 695, L72
Abdo, A. A. et al., 2009b, ApJ, 706, 1331
Abdo, A. A. et al., 2009c, ApJ, submitted
Abdo, A. A. et al., 2009d, Sci, 325, 840
Abdo, A. A. et al., 2009e, Sci, 325, 848
Abdo, A. A. et al., 2009f, ApJ, 696, 1084
Abdo, A. A. et al., 2010a, ApJ, 708, 1254
Abdo, A. A. et al., 2010b, in press
Aharonian, F. et al., 2007, A&A, 472, 489
Atwood, W. B., 2009, ApJ, 697, 1071
Brisken, W. F., Thorsett, S. E., Golden, A. & Goss, W. M., 2003, ApJ, 593, L89
Camilo, F. et al., 2009, ApJ, 705, 1
Camilo, F., Manchester, R. N., Gaensler, B. M., Lorimer, D. L. & Sarkissian, J., 2002, ApJ, 567, L71
D'Amico, N. et al., 2001, ApJ, 552, L45
De Luca, A., Caraveo, P. A., Mereghetti, S., Negroni, M. & Bignami, G. F., 2005, ApJ, 623, 1051
Dodson, R., Legge, D., Reynolds, J. E. & McCulloch, P. M., 2003, ApJ, 596, 1137
Edwards, R. T., Hobbs, G. B. & Manchester, R. N., 2006, MNRAS, 372, 1549
Fierro, J. M. et al., 1993, ApJ, 413, L27
Fomalont, E. B., Goss, W. M., Manchester, R. N. & Lyne, A. G., 1997, MNRAS, 286, 81
Granet, C. et al., 2005, IAPM, 47, 13

Hinton, J. A., Funk, S., Carrigan, S., Gallant, Y. A., de Jager, O. C., Kosack, K., Lemière, A. & Pühlhofer, G., 2007, A&A, 476, L25

Hobbs, G., Lyne, A. G., Kramer, M., Martin, C. E. & Jordan, C., 2004, MNRAS, 353, 1311

Hobbs, G. B., Edwards, R. T. & Manchester, R. N., 2006, MNRAS, 369, 655

Hotan, A. W., van Straten, W. & Manchester, R. N., 2004, PASA, 21, 302

Hui, C. Y. & Becker, W., 2007, A&A, 470, 965

Janssen, G. H. & Stappers, B. W., 2006, A&A, 457, 611

Johnston, S. & Galloway, D., 1999, MNRAS, 306, L50

Johnston, S., Hobbs, G., Vigeland, S., Kramer, M., Weisberg, J. M. & Lyne, A. G., 2005, MNRAS, 364, 1397

Johnston, S., Manchester, R. N., Lyne, A. G., Kaspi, V. M. & D'Amico, N., 1995, A&A, 293, 795

Johnston, S. & Romani, R., 2002, MNRAS, 332, 109

Kanbach, G. et al., 1994, A&A, 289, 855

Kargaltsev, O., Misanovic, Z., Pavlov, G. G., Wong, J. A. & Garmire, G. P., 2008, ApJ, 684, 542

Kaspi, V. M., Lackey, J. R., Mattox, J., Manchester, R. N., Bailes, M. & Pace, R., 2000, ApJ, 528, 445

Keith, M. J., Johnston, S., Kramer, M., Weltevrede, P., Watters, K. P. & Stappers, B. W., 2008, MNRAS, 389, 1881

Kramer, M. et al., 2003, MNRAS, 342, 1299

Manchester, R. N. et al., 2001, MNRAS, 328, 17

Newton, L. M., Manchester, R. N. & Cooke, D. J., 1981, MNRAS, 194, 841

Pellizzoni, A. et al., 2009, ApJ, 691, 1618

Ramanamurthy, P. V., Fichtel, C. E., Kniffen, D. A., Sreekumar, P. & Thompson, D. J., 1996, ApJ, 458, 755

Roberts, M. S. E., Romani, R. W. & Johnston, S., 2001, ApJ, 561, L187

Ruderman, M., Zhu, T. & Chen, K., 1998, ApJ, 492, 267

Shemar, S. L. & Lyne, A. G., 1996, MNRAS, 282, 677

Smith, D. A. et al., 2008, A&A, 492, 923

Standish, E. M., 1998, A&A, 336, 381

Staveley-Smith, L. et al., 1996, PASA, 13, 243

Thompson, D. J. et al., 1992, Nature, 359, 615

Thompson, D. J., Fichtel, C. E., Kniffen, D. A. & Ogelman, H. B., 1975, ApJ, 200, 79

Ulmer, M. P. et al., 1993, ApJ, 417, 738

Wang, N., Manchester, R. N., Pace, R., Bailes, M., Kaspi, V. M., Stappers, B. W. & Lyne, A. G., 2000, MNRAS, 317, 843

Weltevrede, P. et al., 2010, ApJ, 708, 1426

Weltevrede, P. & Johnston, S., 2008a, MNRAS, 387, 1755

Weltevrede, P. & Johnston, S., 2008b, MNRAS, 391, 1210

Weltevrede, P. & Wright, G., 2009, MNRAS, 395, 2117

Weltevrede, P., Wright, G. A. E., Stappers, B. W. & Rankin, J. M., 2006, A&A, 458, 269

Zou, W. Z., Wang, N., Manchester, R. N., Urama, J. O., Hobbs, G., Liu, Z. Y. & Yuan, J. P., 2008, MNRAS, 384, 1063